Indian Journal of Chemical Technology
Vol. 25, January 2018, pp. 9-20

Electrochemical studies on the adsorption interaction and corrosion inhibition properties of a substituted triazinone, BCATDT on mild steel in hydrochloric acid

Shainy K M, Mathew Kuruvilla & Abraham Joseph

Department of Chemistry, University of Calicut, Calicut University P O, Kerala, India.
Email: drabrahamj@gmail.com

Received 24 February 2015; accepted 27 April 2017

A novel triazine based corrosion inhibitor, 6-benzyl-(2-chlorobenzyl) amino 3-thioxo-3, 4-dihydro-1, 2, 4-triazin- (2H)-5-one (BCATDT) has been synthesized and characterized using various spectroscopic techniques. Corrosion inhibition efficiency and other corrosion parameters of BCATDT have been calculated using weight loss measurements, potentiodynamic polarization studies and electrochemical impedance spectroscopy techniques at three different temperatures (303 K, 313 K and 323 K). Among the 0.5 M and 1M HCl solutions 99.55% efficiency is reported for 0.5M solution corresponding to 200 ppm BCATDT. As the acid concentration doubled, only < 7% efficiency decreases even at 323K (92.32%). The potentiodynamic polarization indicates that BCATDT act as an efficient mixed type inhibitor and the most suitable isotherm is found to be the Langmuir adsorption isotherm. The experimental results are then shown to be in conformity with theoretical parameters under B3LYP/6-31G* of Gaussian 03 soft ware. Molecular simulation studies are also performed by Monte Carlo simulation for studying the adsorption of BCATDT on to the various unit cell of iron surface such as Fe (111) Fe (110) and Fe (100) etc.

Keywords: Mild steel, Schiff base, Triazinone, Acid solution, Adsorption, Polarization, EIS

Corrosion inhibition study of mild steel using organic compounds in aqueous and acidic media has got contemporary significance.The excellent mechanical properties and cost effectiveness of mild steel turned it as important constituent material for various industriesand constructions. Acid solutions, particularly hydrochloric acid is employed for the removal of rust and scales in industrial processes. The use of corrosion inhibitors has become one of the most practical methods to control metal dissolution in corrosive media[1-4]. The interaction between the inhibitor and the metal surface plays a crucial role in offering protection to the metal. Inhibitor molecule generally adsorbed on the metal surface and blocking the active sites and hence offer protection to the metal. The adsorption of inhibitors involves the (a) adsorption of anions onto the positively charged metal via electrostatic interaction between the metal/ electrolyte interfaces (b) transfer the protons of acidic molecule to the inhibitor (c) interaction of uncharged inhibitor to the metal surface via chemisorptions and (d) combination of one and two, that is the physisorption of inhibitor molecule on to the metal surface[5,6].

Most of the inhibitors are organic compounds, containing hetero atoms such as N, S, O and P in their aromatic or cyclic structures, multiple bonds, and some functional groups[7-10]. In the recent years Schiff bases also gained attention in the field of corrosion mainly due to the presence of azomethine group of Schiff bases. The corrosion inhibition properties of these compounds are high because of various adsorbing centers available in the molecule and synergistic effect[11-14].

The present study describes the corrosioninhibition efficiency of a Schiff-base 6-benzyl-(2-chloro benzyl)amino)-3-thioxo-3,4-dihydro-1,2,4-triazin-(2H)-5-oneon mild steel in 0.5 and 1M HCl solution att hree different temperatures, which was followed by weight loss studies, electrochemical studies and computational methods. The choice of this Schiff-base is based on the consideration that it contains good π-electron conjugation and number of hetero atoms and therefore enhances its adsorption/coordination onto the mild steel surface.

Experimental Section

Synthesis of inhibitor

The inhibitor 6-benzyl-(2-chloro benzyl)amino)-3-thioxo-3,4-dihydro-1,2,4-triazin-(2H)-5-one was synthesized by a two-step reaction. In the first step the synthesis of 4-amino 3-mercapto 6-phenyl -1,2,4-triazin (2H)-5-one was carried out as per the reported procedure[15,16] and the product was re-crystallized from ethanol.

Then 2-chloro benzyl alcohol (E. Merck 1mol) was then dissolved in absolute alcohol and mixed well by stirring for 5-6 h. The product obtained was purified and re-crystallized.

Characterization of inhibitor

The synthesized inhibitor molecule was characterized by different physico chemical methods. The experimental elemental analysis data were in good agreement with calculated values. CHNS(%) found (calculated) C:55.85 (56.26), H:3.9 (4.21), N:21.74 (20.96), S:8.94 (8.36) C-H-N analyzer (Elementar Vario EL III) SAIF-STIC Cochi. FTIR (KBr); υ: 1746.23 cm^{-1} (C=O stretch), 1241.93 cm^{-1} (C=S stretch), 1667.16 cm^{-1} (C=N stretch), 3297.68 cm^{-1} (N-H stretch), 1545.67 cm^{-1} (N–N stretch), 2923.56 cm^{-1}(C – H stretch)[17,18]. The ^1H NMR spectra in $CDCl_3$ shows chemical shift (δ/ ppm) at δ : 7.0, 2.0 (N–H), 3.84, 3.94 (C–H)[19], FT NMR spectrometer (Bruker Avance III, 400MHz) SAIF-STIC Kochi) . The structure of the compound is shown in Fig. 1.

Materials and methods

The mild steel samples were of thecompositions (wt%), Fe ≈ 98.75%, Mn≈ 1% , C≈ 0.2%, P≈ 0.03%, S≈ 0.02% as evidenced by EDAX spectral method. For electrochemical studies the mild steel samples of 4.8 × 1.9 cm^2 coupons were used, but only 1cm^2 areas were exposed during each measurement. The samples were abraded using different grade of emery papers (600-1200 grade) followed by washing with acetone and distilled water as recommended by ASTM[20].

The medium for the study was prepared from reagent grade hydrochloric acid (E. Merck) and double distilled water. All tests were performed on 303, 313 and 323 K at atmospheric pressure

Weight loss experiments

The weight loss measurements were carried out, in 0.5 M and 1 M HCl solution containing different concentrations of inhibitor for 96 hours at room temperature[21] .The mild steel samples were weighed before and after immersion, and recorded the difference using a precise electronic balance. The variableconcentrations of inhibitor (50, 100, 150, 200 ppm) were used, and it was evidenced that 200 ppm inhibitor offer highest inhibition efficiency in 0.5 M HCl than 1M HCl solution.

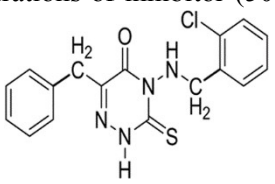

Fig. 1 — Structure of the inhibitor molecule 6-benzyl (2-chloro benzyl) amino)-3-thioxo-3,4-dihydro-1,2,4-triazin-(2H)-5-one

Electrochemical measurements

The electrochemical impedance (EIS) and potentio dynamic polarization studies were carried out using Gill AC instruments (ACM, UK model no.1745) and the data were analyzed using Gill AC software. The instrumentconsists of a three electrode corrosion cell with platinum, used as the auxiliary electrode and saturated calomel electrode as the reference electrode. The working electrode was immersed into the test solution for 60 min to establish a steady state open circuit potential. The EIS measurements were carried out in a frequency range 0.1 to 10000 Hz with amplitude 10 mV. The polarization measurements were recorded with a scan rate of 1 mV/S in the potential range from -250 to 250 mV.

Adsorption studies

The adsorption of inhibitor molecule on the metal surface plays a major role in its corrosion inhibition mechanism. Various adsorption isotherms like Langmuir, Temkin, Fremkin, Freundlich were tested and, among them Langmuir was found to be the best, giving a straight line graph. The value of regression coefficients (R^2) confirmed the validity of the isotherm.

Surface characterization

The surface characterization of metal was carried out by scanning electron microscopy (SEM). The surface morphology of the samples wererecordedin the presence and absence of inhibitor. The study was conducted using a Hitachi model SU 6600 scanning electron microscope at NIT Calicut, Kerala, India. All micrographs were recorded at a 500x magnification

Quantum chemical calculation

The quantum chemical calculations were performed with complete geometry optimization of the inhibitor molecule using a standard Gaussian 03 software package. The B3LYP (Becke's three –parameter hybrid function) was combined with Lee Yang and Parr (LYP)) and was employed in DFT calculations using 6-31G* basis set .The energies of the frontier molecular orbital (HOMO and LUMO) used to calculate and interpret the adsorption and characterization of the inhibitor molecule[22].

Results and Discussion

Weight loss measurements

The weight loss of the mild steel samples due to corrosion obtained from the different concentrations

Table 1 — Percentage inhibition efficiency obtained by weight loss of mild steel in 0.5 and 1M HCl containing various concentrations of the inhibitor BCATDT at 303 K

Acid conc.(M)	Inhibitor conc.(ppm)	% Inhibition efficiency with time in hr			
		24	48	72	96
0.5	Blank	-----	-----	-------	------
	50	75.01	74.52	73.89	72.50
	100	96.68	95.44	95.35	95.03
	150	97.44	96.21	96.11	95.86
	200	98.99	98.52	98.06	97.97
1	Blank	-------	-------	-------	------
	50	83.42	83.00	82.16	82.01
	100	94.21	93.77	93.62	93.13
	150	95.06	94.91	94.36	94.11
	200	97.33	97.08	96.78	96.25

and temperatures are listed in Table 1. The inhibition efficiency (IE)were calculated from equation[23] (1).

$$IE\ \% = \frac{W_0 - W}{W_0} \times 100 \quad \ldots (1)$$

where W_0 and W are the weight loss of steel without and with inhibitor

BCATDT shows higher inhibition efficiency at 200 ppm (99.55%). The increase in corrosion rate was more pronounced with the rise in temperature for uninhibited and inhibited acid solution.

Electrochemical impedance spectroscopy

The electrochemical impedance spectroscopy is a widely used tool for the investigation of corrosion inhibition process. This technique is based on the measurement of impedance of double layer at the metal / solution interface. The equivalent circuit diagram is represented in insight of Fig. 2 (a).The impedance measurements were carried out after the immersion of 60 min in 0.5 M and 1M hydrochloric acid solution in the absence and presence of different concentrations of inhibitor. The impedance spectra exhibits a single semi circle for a particular concentration, called Nyquist plots, and a representation of the same is given in Fig. 2 at 303, 313 and 323 K respectively. The diameter of the semi circle increases with increase in inhibitor concentration and the slightly depressed nature of the semi circle are due to the frequency dispersion as a result of the roughness and inhomogenity of the electrode surface[24]. The electrochemical corrosion kinetic parameters namely, double layer capacitance (C_{dl}) and charge transfer resistance (R_{ct}), were calculated from the Nyquist plots and are listed in Tables 2, 3 and 4 corresponding to temperatures 303, 313 and 323 K respectively. IE % was calculated from the equation,

$$\text{IE } \% = \frac{R_{ct^*} - R_{ct}}{R_{ct^*}} \times 100 \quad \ldots (2)$$

where R_{Ct^*} and R_{Ct} are the charge transfer resistance of mild steel with and without inhibitor.

The values of R_{ct} and C_{dl} exhibit opposite trends, the increase in corrosion current indicate a strong surface coverage by the inhibitor. On the other hand, the values of C_{dl} decreases with increasing inhibitor concentration due to a decrease in the dielectric constant or anincrease in the thickness of protective layer, suggesting a strong adsorption on to the metal surface. The system offers good inhibition efficiency of 99.55% at 200 ppm with inhibitor due to these excellent adsorption characteristics.

Potentiodynamic polarization

The corrosion behavior of mild steel in 0.5 and 1M hydrochloric acid was investigated by the potentiodynamic technique, at different temperatures and the resulting plots are given in Fig. 3. The potentiodynamic polarization studies carried out gather the information of cathodic and anodic reactions. The values of electrochemical parameters namely, corrosion potential (E_{corr}) and Tafel slopes (β_a and β_c), were obtained from the Tafel polarization curves are listed in the Tables 5, 6 and 7 for various temperatures. The IE % was calculated from the equation (3)[26,26].

$$\text{IE } \% = \frac{I_{Corr^*} - I_{Corr}}{I_{Corr^*}} \times 100 \quad \ldots (3)$$

where $I_{corr}{}^*$ and I_{corr} are the corrosion current densities of the inhibited and uninhibited solutions

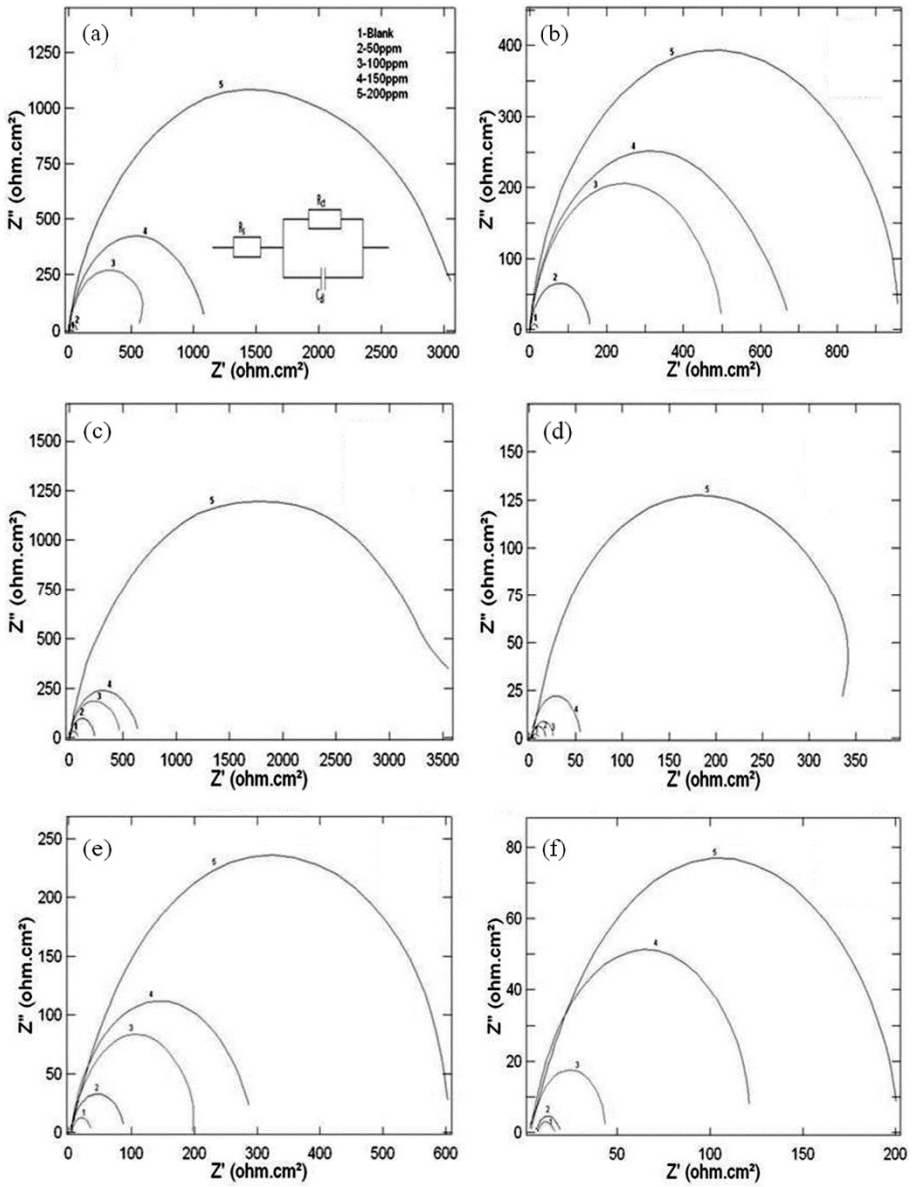

Fig. 2 — Nyquist plots for mild steel corrosion in (a) and (b) for 303 K (c) and (d) for 313 K, (e) and (f) for 323 K in the presence and absence of different concentrations of inhibitorBCATDT in 0.5 and 1 M HCl

Table 2 — Electrochemical impedance data for mild steel corrosion in different concentration of HCl in the presence and absence of inhibitor BCATDT at 303 K

Acid conc.(M)	Inhibitor conc.(ppm)	R_{ct} (Ω cm^2)	C_{dl}(μF)	I_{corr}(mA/cm^2)	C R (mils/yr)	% IE
0.5	Blank	13.87	127.50	1.8780	857.00	----
	50	59.14	69.43	0.4411	194.60	76.54
	100	638.30	33.07	0.0040	18.65	97.82
	150	1044.40	14.24	0.0024	11.14	98.67
	200	2899	7.80	0.0089	4.10	99.55
1	Blank	18.54	132.90	1.4070	642.00	---
	50	154.00	53.90	0.1694	77.30	87.96
	100	497.30	30.28	0.0052	23.94	96.27
	150	631.40	18.84	0.0041	18.85	97.06
	200	975.30	10.05	0.0026	12.20	98.09

Table 3 — Electrochemical impedance data for mild steel corrosion in different concentrations of HCl in the presence and absence of inhibitor BCATDT at 313 K

Acid conc.(M)	Inhibitor conc.(ppm)	R_{ct} (Ω cm^2)	C_{dl} (μF)	I_{corr} (mA/cm^2)	C R (mils/yr)	% IE
0.5	Blank	71.88	99.48	0.3629	165.60	----
	50	252.20	106.70	0.1034	47.20	71.49
	100	452.30	39.61	0.0057	26.32	84.10
	150	623.80	27.72	0.0048	19.08	88.47
	200	3341	10.91	0.0007	3.56	97.85
1	Blank	10.30	1437	2.5330	1156	----
	50	18.46	263	1.4130	644.80	44.20
	100	56.51	426.50	0.9846	449.00	61.14
	150	85.33	239.90	0.3057	139.50	87.92
	200	381.30	40.19	0.0068	31.22	97.29

Table 4 — Electrochemical impedance data for mild steel corrosion in different concentrations of HCl in the presence and absence of inhibitor BCATDT at 323 K

Acid conc.(M)	Inhibitor conc.(ppm)	R_{ct} (Ω cm^2)	C_{dl} (μF)	I_{corr} (mA/cm^2)	C R (mils/yr)	% I E
0.5	Blank	30.70	132.50	0.8497	389.70	-----
	50	87.34	102.20	0.2987	136.30	64.85
	100	224.90	78.42	0.1660	52.93	86.34
	150	290.60	47.13	0.0089	40.96	89.43
	200	743.60	37.99	0.0035	16.01	95.87
1	Blank	9.40	920.30	2.7720	1265	-----
	50	14.33	496.40	1.8200	830.70	34.40
	100	43.10	110.10	0.6053	276.20	78.19
	150	134.70	87.61	0.1937	88.37	91.02
	200	299.60	128.70	0.0870	39.73	92.32

The results show that the percentage inhibition efficiency increases with increase in concentration of inhibitor and is parallel with those obtained from electrochemical impedance measurements at different concentrations and temperatures studied. The shift of Tafel lines to less negative potential values indicate decrease in the corrosion rate in the presence of inhibitor. In acidic solution, anodic reaction involves the passage of metal ion from the metal solution and the cathodic reaction is the discharge of H^+ ions to hydrogen gas or reduced oxygen. An inhibitor might affect either anodic or cathodic reactions or both in some cases. In this case the inhibitor, affect anodic and cathodic polarizations and shifted both the values to lower current densities, thus the inhibitor BCATDT act as mixed type inhibitor[27,28].

Adsorption behaviour

The inhibitor molecules were adsorbed on the metal surface when the interaction between the inhibitor molecules and metal surface are higher than that of water molecule and metal surface. Different adsorption isotherms were plotted and Langmuir isotherm was found to be the best description of this adsorption behaviour (Fig. 4).

The Langmuir adsorption can be represented by the equation

$$C/\theta = 1/K_{ads} + C \quad \ldots (4)$$

where θ is the degree of surface coverage, K_{ads} is the adsorption equilibrium constant and C is the concentration of the inhibitor in mole/litre in bulk solution.

The equilibrium constant (K_{ads}) for the adsorption process were related to the standard free energy of adsorption (ΔG^0_{ads}) by the expression

$$\Delta G^0_{ads} = - 2.303\ RT \log (55.5\ K_{ads}) \quad \ldots (5)$$

where ΔG^0_{ads} is the Gibbs free energy of adsorption, T is the temperature in Kelvin and 55.5 is the molar concentration of water in solution. The negative values of ΔG^0_{ads} ensure the spontaneity of the adsorption process and the stability of adsorbed layer on the metal

surface. It is reported that, if the values of ΔG^0_{ads} is around -20 kJ /mol or lower, then weak electrostatic interaction (physisorption) exist between the metal surface and inhibitor molecule and if the value comes around -40 kJ/mol or higher which indicates the charge transfer or covalent bonding (chemisorptions) exist between the metal and inhibitor molecule. TheΔG^0_{ads}valuesof the inhibitor BCATDT is around -

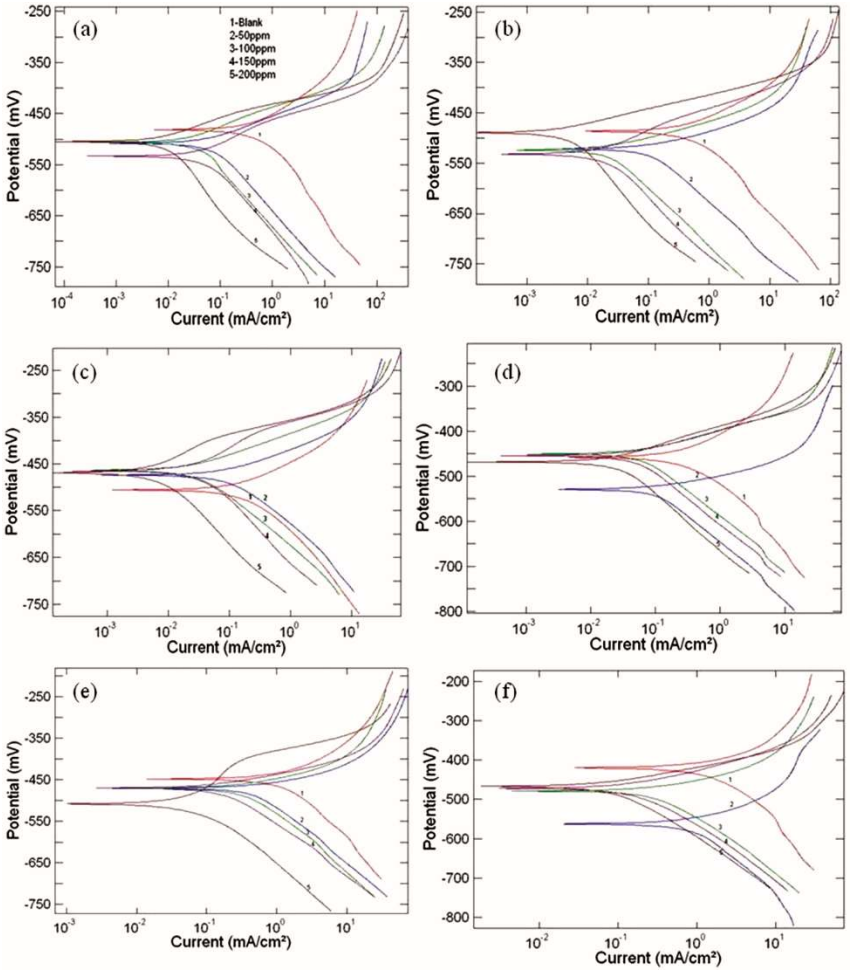

Fig. 3 — Polarization plots for mild steel corrosion in (a) and (b) for 303 K (c) and (d) for 313 K, (e) and (f) for 323 K in the presence and absence of different concentrations of inhibitor BCATDT in 0.5 and 1 M HCl

Table 5 — Polarization parameter and corresponding inhibition efficiency for the corrosion of mild steel at various concentrations of inhibitor BCATDT at 303 K

Acid conc.(M)	Inhibitor conc.(ppm)	E_{corr} (mV)	β_a (mV/dec)	β_c (mV/dec)	I_{corr} (mA /cm^2)	C R (mils/yr)	% IE
0.5	Blank	-483.93	48.97	63.37	0.3253	148.45	-------
	50	-526.01	29.03	64.47	0.0755	34.49	76.79
	100	-523.43	21.75	43.48	0.0099	4.54	96.95
	150	-480.47	33.90	47.42	0.0079	3.63	97.57
	200	-485.37	19.52	26.47	0.0011	0.53	99.66
1	Blank	-482.27	57.93	71.12	0.3330	151.94	----
	50	-508.02	32.11	59.90	0.0382	17.45	88.52
	100	-508.12	29.37	32.83	0.0141	6.45	95.76
	150	-508.12	24.89	174	0.0108	4.96	96.77
	200	-498.99	21.42	23.66	0.0066	3.09	97.98

Table 6 — Polarization parameter and corresponding inhibition efficiency for the corrosion of mild steel at various concentrations of inhibitor BCATDT at 313 K

Acid conc.(M)	Inhibitor conc.(ppm)	E_{corr} (mV)	β_a (mV/dec)	β_c (mV/dec)	I_{corr} (mA / cm^2)	C R (mils/yr)	% IE
0.5	Blank	-483.93	48.97	63.37	0.3253	148.45	-----
	50	-476.01	29.03	64.47	0.0755	34.49	76.01
	100	-473.43	21.75	43.48	0.0099	4.54	96.38
	150	-480.47	33.90	47.42	0.0079	3.63	97.62
	200	-485.37	19.52	26.47	0.0011	0.53	99.02
1	Blank	-449.60	39.25	49.07	0.4700	214.50	----
	50	-474.24	24.57	58.78	0.2597	118.50	44.74
	100	-470.51	31.40	71.06	0.1922	87.69	59.12
	150	-473.04	21.07	26.09	0.0555	25.33	88.19
	200	-507.18	36.29	36.02	0.0169	7.74	96.38

Table 7 — Polarization parameter and corresponding inhibition efficiency for the corrosion of mild steel at various concentrations of inhibitor BCATDT at 323 K

Acid conc.(M)	Inhibitor conc.(ppm)	E_{corr} (mV)	β_a (mV/dec)	β_c (mV/dec)	I_{corr} (mA /cm^2)	C R (mils/yr)	% IE
0.5	Blank	-459.83	61.13	69.67	0.2119	148.71	-----
	50	-525.20	25.21	92.81	0.0725	33.09	66.12
	100	-451.99	32.82	60.84	0.0364	16.63	82.35
	150	-451.82	20.82	32.34	0.0175	8.02	91.01
	200	-468.48	36.33	45.77	0.0117	5.37	94.61
1	Blank	-421.43	43.94	59.76	0.6188	282.39	----
	50	-462.38	37.11	54.11	0.3778	172.43	38.94
	100	-469.13	26.37	74.85	0.1207	55.11	80.49
	150	-468.69	42.83	73.09	0.8799	34.64	87.73
	200	-464.26	36.77	67.77	0.0414	18.89	93.30

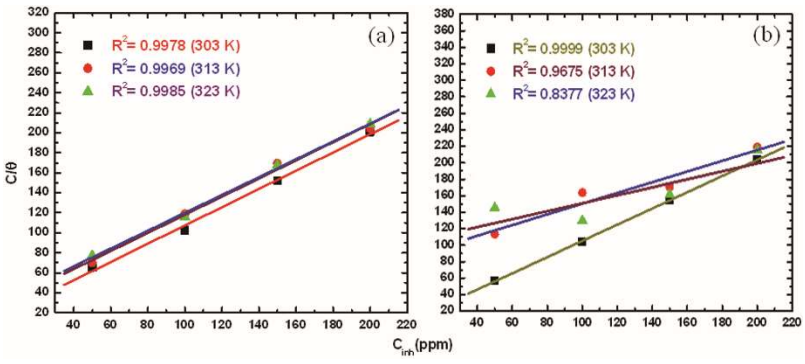

Fig. 4 — Langmuir adsorption isotherms for the different concentrations of inhibitorBCATDTat 303 K,313 K and 323 K at (a) 0.5 M and (b) 1M HCl

40 kJ/mol, which indicates that chemisorptions occur on the metal surface[29,30]. The equilibrium constant K_{ads} and the corresponding free energy of adsorption ΔG^0_{ads} were tabulated and are given in Table 8.

SEM analysis

SEM images of the steel samples were recorded to observe the changes that occurred on the surface during the corrosion in the presence and absence of the inhibitor. The mild steel samples, highly damaged due to the direct attack of 0.5 M and 1M hydrochloric acid solution are represented by Fig. 5 (a) and (b) respectively. This type of corrosion is typical in aggressive acid solutionsand the surface becamesmoothafter the addition of 200 ppm inhibitor to the 0.5 and 1M HCl solutions (Fig. 5 (c) and (d)) . It is clear that the irregularities on the metal surface due to corrosion are absent when the metal surface is exposed in acid solution containing the inhibitor. This result reveals

Table 8 — Estimation of the Equilibrium Adsorption Constant (K_{ads}) and the Free Energy of Adsorption (ΔG^0_{ads}) of the BCATDT on mild steel –HCl system at various temperatures and concentrations

HCl	Temp (K)	50ppm ΔG^0_{ads} (kJ mol^{-1})	K_{ads} (mol^{-1})	100ppm ΔG^0_{ads} (k J mol^{-1})	K_{ads} (mol^{-1})	150ppm ΔG^0_{ads} (k J mol^{-1})	K_{ads} (mol^{-1})	200ppm ΔG^0_{ads} (k J mol^{-1})	K_{ads} (mol^{-1})
0.5M	303	-35.24	2347.12	-40.14	1661.18	-40.35	1809.46	-43.77	6374.26
	313	-36.13	1928.87	-36.10	1902.62	-36.05	1871.46	-39.05	7984.49
	323	-36.36	1367.52	-37.65	2209.66	-37.35	1973.39	-38.75	3333.33
1M	303	-37.20	5147.92	-38.20	9284.04	-38.32	8052.09	-38.60	9009.82
	313	-33.13	6093.13	-32.92	5659.49	-35.89	1775.15	-39.21	6298.31
	323	-33.15	4142.01	-36.33	1353.20	-38.68	3240.41	-39.38	4210.52

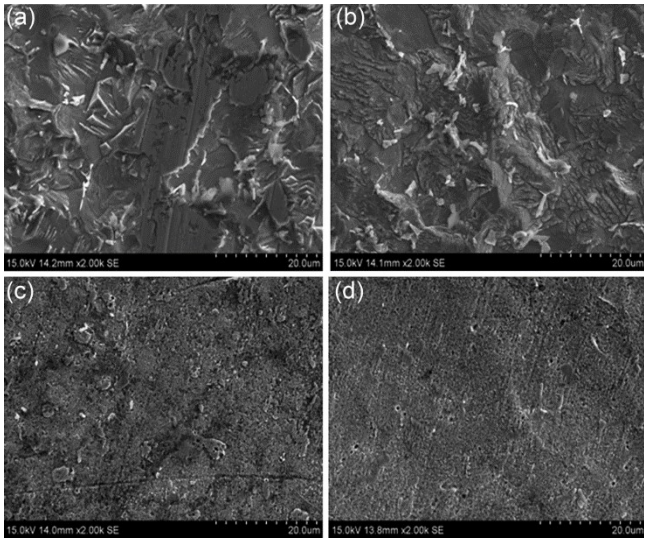

Fig. 5 — SEM micrographs of the mild steel after the immersion in without BCATDT(a) 0.5M HCl,(b) 1M HCl , showing the damaged surface in acid solution, and(c) and (d) with BCATDT, showing the inhibited smooth surface

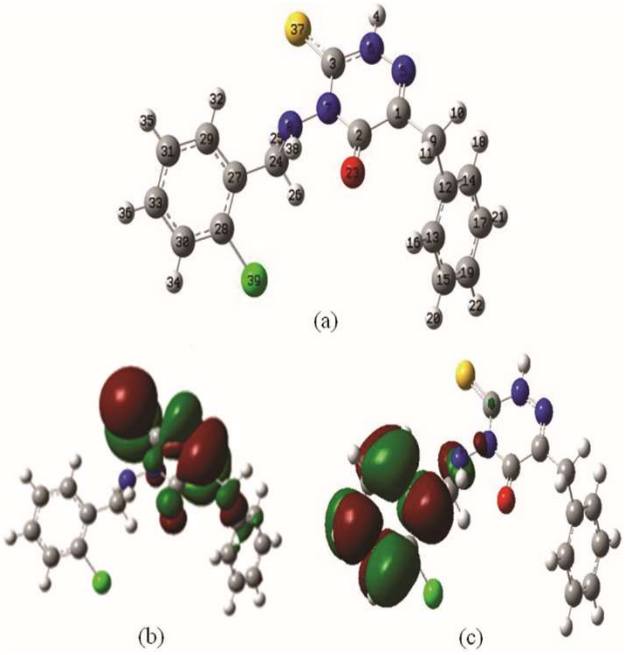

Fig. 6 — Optimized molecular structure of the inhibitor BCATDT, (b) highest occupied molecular orbital HOMO (c) lowest unoccupied molecular orbital LUMO

that the protective layer formed on the surface by adsorption or coordination does offer excellent corrosion protection properties.

Computational studies

According to Frontier molecular orbital theory, HOMO and LUMO of a reacting species plays a major role in predicting the reactivity of the inhibitor molecule. When the values of E_{HOMO} increase, that facilitates better adsorption and enhances the inhibition efficiency[31,32]. Similarly lower values of E_{LUMO} indicate the possibility of a molecule to accept electrons. The energy difference between HOMO and LUMO is ΔE ($\Delta E = E_{LUMO} - E_{HOMO}$). Lower the value of ΔE, better will be the inhibition efficiency, and higher value reveals lower inhibition efficiency. In addition to that a larger value of the energy gap indicates low reactivity to the metal surface, because the energy gap is related to the softness or hardness of a molecule. A soft molecule is more reactive than a hard molecule because a hard molecule has a larger energy gap[33-35]. Figure 6 express (a) the optimized geometry of BCATDT and (b), (c) are the pictorial representations of HOMO and LUMO.

In Hartree-Fock theory a good relationship exist between E_{HOMO} and E_{LUMO}, with the ionization potential (IP), electron affinity (EA), as E_{HOMO} = -IP and E_{LUMO} = -EA. This is predicted on the basis of Koopmans theorem. In a similar way Janak's theorem holds in the case of pure KS-DFT method. Even though the B3LYP method is not pure DFT the HOMO and LUMO Eigen values obtained from it matches well with electrochemically extrapolated IP and EA values[36]. Here in we also assume E_{HOMO} as -IP and E_{LUMO} as –EA, then the electro negativity

$$-\mu = \frac{I+A}{2} = \chi \quad \ldots (6)$$

$$\eta = \frac{I-A}{2} \quad \ldots (7)$$

When the two systems are in contact, the electron flows from inhibitor (lowerχ) to the metal (higherχ) until the chemical potential become equal[37]. Table 9 represent the quantum chemical parameters related to molecular structure (energies of neutral, cationic and anionic forms, and energies of HOMO and LUMO of neutral molecule of BCATDT), ionization potential, electron affinity, dipole moment (μ), electro negativity (χ), global hardness (η), global softness (σ=1/η) and global nucleophilicity (N) etc. The global nucleophilicity descriptors largely focus on the energies and populations of frontier orbitals of the reactants, requiring calculations on chemical potential[38] and Fukui functions[39], in addition to the frontier molecular orbitals (FMO)[40,41]. The global nucleophilicity directly related to the basic character of molecule, hence the BCATDT can act as an excellent corrosion inhibitor towards mild steel.

$$\text{Global Nucleophilicity, N} = \frac{16(I-A)}{(3I+A)^2} \quad \ldots (8)$$

The local reactivity was analyzed by means of condensed Fukui function. The natural atomic orbital (NAO) charges obtained from natural population analysis (NPA) are used for finding Fukui functions. The electron density in the electrophilic and nucleophilic Fukui functions (f^+ and f^-) can be calculated using the finite difference approximation using equation (9) and (10),

Table 9 — Quantum chemical parameters of BCATDT

BCATDT	
$E_{neutral}$(eV)	-49237.21
E_{anion} (eV)	-49237.75
E_{cation}(eV)	- 49229.59
HOMO(eV)	-6.25
LUMO(eV)	-2.16
I (eV)	6.25
A (eV)	2.16
μ (Debye)	1.31
χ(eV)	4.25
η(eV)	2.04
σ	0.49
I-A	4.09
16(I-A)	65.4176
3I+A	20.9198
Sq(3I+A)	437.638
N	0.1494

$$f^+(r) = (\delta\rho(r)/\delta N)^+\upsilon = q_{(N+1)}(r) - q_{(N)}(r) \quad \ldots (9)$$

$$f^-(r) = (\delta\rho(r)/\delta N)^-\upsilon = q_{(N)}(r) - q_{(N-1)}(r) \quad \ldots (10)$$

where ρ, q (N+ 1), q (N-I) and q (N) are the density of electrons and the NAO charges of the atom r, in cationic, anionic, neutral systems of BCATDT

When the molecule acts as a nucleophile, the value of f^+ is maximum. The site for the electrophilic attack is controlled by the value of f^-. It is clear that the most reactive sites for the electrophilic attack in the present molecule BCATDT are S_{37}, N_8, N_7, N_5 and C_3, which are more susceptible for adsorption on to the metal surface, and the local reactivity of these atoms are also higher than others, which again confirm the higher inhibition efficiency. Table 10 represent the Fukui

Table 10 — Nucleophilic and electrophilic Fukui functions of BCATDT

Atom no.	f^-	f^+
C 1	0.0008	0.2090
C 2	0.0027	0.1506
C 3	0.0145	0.0230
H 4	0.0051	0.0000
N5	0.0127	0.2951
N6	0.0098	0.0485
N7	0.0145	0.0887
N8	0.0488	0.0122
C9	0.0012	0.0017
H10	0.0001	0.0041
H11	0.0002	0.0039
C12	0.0005	0.0106
C13	0.0004	0.0045
C14	0.0005	0.0056
C15	0.0003	0.0005
H16	0.0000	0.0001
C17	0.0001	0.0006
H18	0.0000	0.0001
C19	0.0008	0.0057
H20	0.0000	0.0001
H21	0.0000	0.0001
H22	0.0000	0.0000
O23	0.0078	0.1042
C24	0.0052	0.0065
H25	0.0022	0.0005
H26	0.0010	0.0016
C27	0.0011	0.0015
C28	0.0025	0.0001
C29	0.0005	0.0009
C30	0.0013	0.0003
C31	0.0032	0.0001
C32	0.0004	0.0001
C33	0.0007	0.0003
H34	0.0000	0.0000
H35	0.0000	0.0000
H36	0.0000	0.0000
S37	0.8321	0.0189
H38	0.0004	0.0002
Cl39	0.0015	0.0001

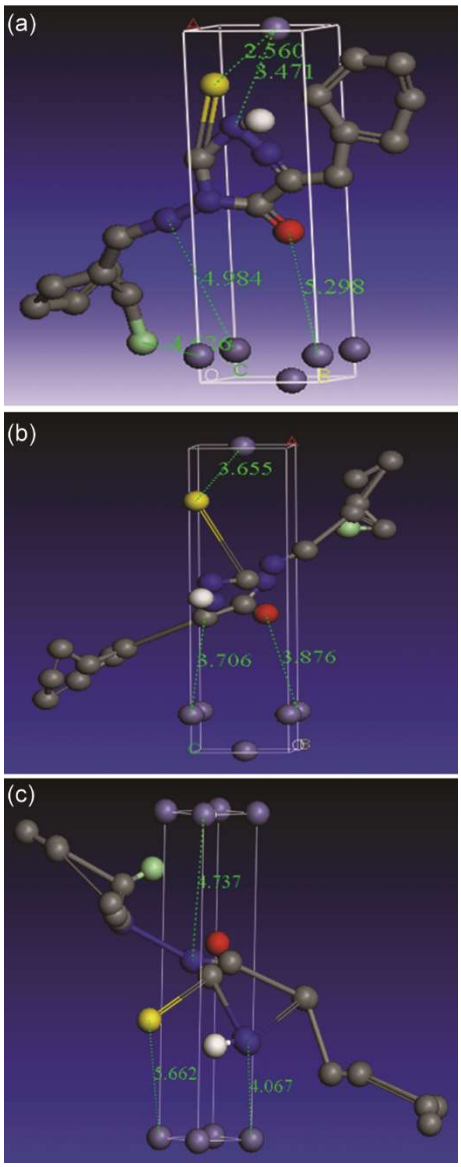

Fig. 7 — Simulation diagram for (a) Fe (111), (b) Fe (110) and (c) Fe (100) surface

functions for nucleophilic (f^-) and electrophilic (f^+) character of BCATDT.

Molecular simulation studies

The molecular simulation study was performed using the Monte Carlo simulation method. The adsorption energy, deformation energy, and the sum of the rigid adsorption energy for BCATDT were calculated. The corresponding simulation diagram for (a) Fe (111), (b) Fe (110) and (c) Fe (100) are given in Fig. 7. Charge transfer processes exist between a good inhibitor molecule and the metal surface. Robust corrosion inhibition depends on the ease with which the inhibitor can transfer electrons to the vacant orbital of the metal and the ease with which it can accept free electrons from the metal surface. The charge distributions on the molecule BCATDT were worked out under DFT/B3LYP/6-31G*.

Table 11— Adsorption parameters of BCATDT

Adsorption parameters	Fe(111)	Fe(110)	Fe(100)
Total energy (kcal/mol)	-2657.8116	-7540.129	-1435.35
Adsorption energy (kcal/mol)	-334.4502	-724.0926	-113.5932
Rigid adsorption energy (kcal/mol)	1795.6414	5764.2190	8721.9750
Deformation energy (kcal/mol)	-2130.0921	1476.7070	-2637.3470
dE_{ads}/dN_i (kcal/mol)	-334.4502	-724.0926	-113.5932

The simulations indicate that the BCATDT molecule gets adsorbed on the iron surface most frequently through interactions involving the sulphur atoms (2.560) and nitrogen atoms (3.471). Both interactions can help form to coordinate bond with the Fe atom of mild seel surface. Among the three kinds of Fe surfaces (100), (110), (111), the Fe (111) surface is found to have greater stability so it is chosen to simulate the adsorption process[42,43].

The total energy of the substrate- adsorbate system is defined as the sum of the energy of the adsorbatemolecule, the deformation energy and the rigid adsorption energy. The surface energy for iron (substrate) is taken to be zero. The adsorption energy is the energy released (or required) when the relaxed adsorbate components are adsorbed on to the iron surface[44]. The deformation energy is the energy released when the adsorbed inhibitor is relaxed on the iron surface. The calculated total energy, rigid adsorption energy, deformation energy and dE_{ad}/dN_i (the energy of substrate–adsorbate system where one of the adsorbate components has been removed), corresponding to Fe (111) are given in Table 11.

Conclusion

The BCATDT acts as effective corrosion inhibitor for mild steel in 0.5M and 1M hydrochloric acid. The inhibition efficiencies measured through weight loss, electrochemical impedance spectroscopy and Tafel polarization studies show thatthe results are in good agreement with each other**.** The inhibition efficiency was found to depend on the number of adsorption sites and charge density of the inhibitor molecule.

(1) The inhibitor molecule shows very goodinhibition efficiency for mild steel in 0.5 and 1Mhydrochloric acid at room temperature (303 K) and moderate inhibition efficiency at high temperature (313 K and 323 K).
(2) The polarization measurements indicate that the compound can resist both anodic and cathodic reaction, thus it acts as a mixed type inhibitor.
(3) The adsorption process was confirmed by chemisorptions on the mild steel surface and obeyed the Langmuir adsorption isotherm.
(4) The surface characterization gave information about the corrosion inhibition due to strong coordination between the metal and the inhibitor.
(5) The compound is a good inhibitor in the presence of electron attracting chlorine atom, which decrease electron donating ability of the vacant d-orbital of the metal by its inductive effect (-I) and also decrease the delocalization of π-electrons on the ring. The effect of chlorine atom in the compound could be neutralized by the presence of enough hetero atom and hence it can behave as a good corrosion inhibitor in mild steel-hydrochloric acid system.
(6) The results of quantum chemical studies show that local reactivity of atoms and global nucleophilicity supports the better adsorption characteristics of the inhibitor BCATDT.
(7) Monte Carlo simulations indicate that the BCATDT molecule gets adsorbed on to the iron surface mostly through interactions that involve sulphur atoms and nitrogen atoms. Both these interactions can help to form coordinate bond with the Fe atom. Among the three kinds of Fe surfaces (100), (110), (111), the Fe (111) surface is found to have greater stability and is chosen to simulate the adsorption process.

Acknowledgement

The authors are very much grateful to Dr. Anup V. Thomas, Asst. Professor, SCET, Trivandrum for extending the facilities for computational calculations and Kerala State Council for Science Technology and Environment (KSCSTE) for offering instrumentation facility

References

1 Quraishi M A, Ishtiaque Ahamad, Singh Ashish Kumar, Shukla Sudhish Kumar, Lal B & Singh Vakil, *Mater Chem Phys*, 112 (2008) 1035.
2 Fontana M G & Greene N D, *Corros Eng*, 1984.
3 Seung-Hyun Yoo, Young-Wun Kim, Keunwoo Chung, Nam-Kyun Kim & Joon-Seop Kim, *Ind Eng Chem Res*, 52 (2013) 10880.
4 AngH L, Liu R B & Xin J, *Corros Sci*, 46 (2004) 2455.
5 Amin M A, Abd El Rehim S S, El-Sherbini E E F & BayoumiR S, *Electrochim Acta*, 52 (2007) 3588.
6 Shokry H, Yuasa M, Sekine I, Issa R M, El-Baradie H Y & Gomma G K, *Corros Sci*, 40 (1998) 2173.
7 Yin Yan, Weihua Li, Lankun Cai & Baorong Hou, *Electrochim Acta*, 53 (2008) 5953.
8 Quraishi M A & Jamal D, *J Appl Electrochem*, 32 (2002) 425.
9 Ehteshamzadeh M, Jafari A H, Esmaeel Naderi & Hosseini M G, *Mater Chem Phys*, 113 (2009) 986.
10 Hui-Long Wang, Hong-Bo Fan & Jia-Shen Zheng, *Int J Electrochem Sci*, 7 (2012) 11884.
11 Aysel Yurt, Berrin Duran & Hakan Dal, *Arab J Chem*, 7 (2014) 732
12 Mohsen Lashgari, Mohammad-Reza Arshadi & Somaieh Miandari, *Electrochim Acta*, 55 (2010) 6058.
13 Bentiss F, Lagrenee M, Traisnel M & Hornez J C, *Corros Sci*, 41 (1999) 789.
14 Sam John & Abraham Joseph, *RSC Adv*, 2 (2012) 9944.
15 John S, Joseph B, Aravindakshan K K & Joseph A, *Mater Chem Phys*, 122 (2012) 374.
16 Khedr A M & Marwani H M, *Int J Electrochem Sci*, 7 (2012) 10074.
17 Cain J P, Gassman P L, Wang H & LaskinA, *Phys Chem Chem Phys*, 12 (2012) 5206.
18 Abd El Rehim S S, Ibrahim M A M & Khalid K F, *Mater Chem Phys*, 70 (2001) 268.
19 ASTM G-31-72, Standard recommended Practice for the laboratory immersion corrosion testing of metals, (1990) 401.
20 Volovitch P, GazizzullinI, Ruel F & Ogle K, *Corros Sci*, 53 (2011) 1362.
21 Frisch M J, Trucks G W & Schlegel H B, Gaussian 03, revision B 03 Pittsburgh, Pa Gaussian Inc (2003).
22 Sorkhabi H A, Shaabani B & Seifzdeh D, *Electrochim Acta*, 50 (2005) 3446.
23 Khaled K F & Hackerman N, *Electrochim Acta*, 48 (2003) 2715.
24 Abd El-Maksoud S A, *Int J Electrochem Sci*, 3 (2008) 528.
25 Saravana Loganathan Asok Kumar, Mayakrishnan Gopiraman, Moorthy Saravana Kumar & Anandaram Sreekanth, *Ind Eng Chem Res*, 50 (2011) 7824.
26 Lebrini M, Bentiss F, Vezin H & Lagrenee M, *Appl Surf Sci*, 252 (2005) 950.
27 Olivares-XometlO, Likhanova N V, Dominguez-AguilarM A, Hallen J M, Zamudio L S &Arce E, *Appl Surf Sci*, 252 (2006) 2139.
28 Issaadi S, Douadi T, Zouaoui A, Chafaa S, Khan M A & BouetG, *Corros Sci*, 53 (2011) 1484.
29 Liu S, Duan M, Jiang R Y , Feng Z P & Xiao R, *Mater Corros*, 60 (2009) 9999.
30 Lopez D A, SimisonS N & De Sanchez S R, *Electrochim Acta*, 48 (2003) 845.
31 Ebenso E E, Arslan T, Kandemirli F, Caner N & Love I, *Int J Quantum Chem*, 110 (2010) 1003.
32 Fukui K, Yonezawa T & Shingu H A, *J Chem Phys*, 20 (1952) 722.
33 El Ashry H E, El Nemr A, Esawy S A & Ragab S, *Electrochim Acta*, 51 (2006) 3957.
34 Eddy N O, *Mol Simul*, 36 (2010) 354.

35 Anup T &Bhanuprakash K, *Chem Phys Chem*, 13 (2012) 597.
36 Li W, Zhao X, Liu F, Deng J & Hou B, *Mater Corros*, 60 (2009) 287.
37 Parr R G, Donnelly R A & Palke W E, *J Chem Phys*, 68 (1978) 3801.
38 Parr R G & Yang W, *J Am Chem Soc*, 106 (1984) 4049.
39 Fukui K, Yonezawa T & Nagata C, *J Chem Phys*, 22 (1954) 1433.
40 Young H Jhon, Jae-Goo Shim, Jun-Han Kim, Ji Hyun Lee & Kyung-Ryong Jang Jaheon Kim, *J Phys Chem A*, 114 (2010)12907.
41 Satoh S, Fujimoto H & Kobayashi H, *J Phys Chem B*, 110 (2006) 4846.
42 Khaled K F, *Electrochim Acta*, 53 (2008) 3484.
43 Khaled K F, *Electrochim Acta*, 48 (2003) 2493.